Journal of Materials Chemistry C

Accepted Manuscript

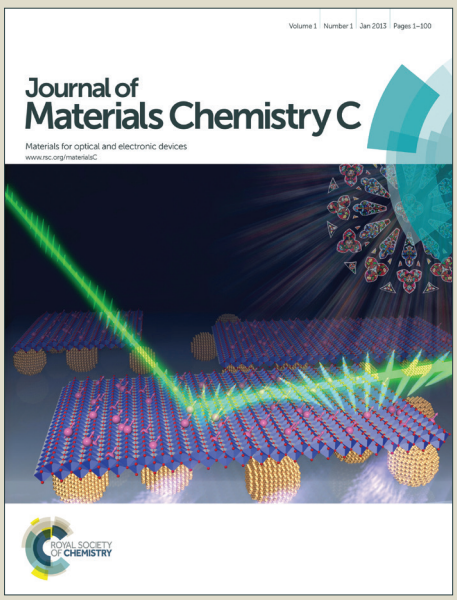

ROYAL SOCIETY OF CHEMISTRY

www.rsc.org/materialsC

Cite this: DOI: 10.1039/c0xx00000x

www.rsc.org/xxxxxx

ARTICLE TYPE

Ordered Array based on Vapor-Processed Phthalocyanine Nanoribbons

Qiubing Min[a], Xiaoli Zhao[a], Bin Cai[a], Yan Liu[a], Qingxin Tang*[a] ,Yanhong Tong*[a], Wenping Hu*[b], Yichun Liu[a]

Received (in XXX, XXX) Xth XXXXXXXXX 20XX, Accepted Xth XXXXXXXXX 20XX

DOI: 10.1039/b000000x

The ordered arrays of the CuPc/F_{16}CuPc nanoribbons have been formed by two different methods, in situ vapor growth method, and a pushing transfer method based on the vapor grown bundle-like nanoribbons. The low deposition temperature and the low vapor concentration are critical for the growth of the small-size nanoribbons. During the growth process the external moment of the small-size nanoribbon gradually increases, which helps to bend and adhere the slim nanoribbon to the substrate surface, thus leading to the formation of in situ grown CuPc/F_{16}CuPc single-crystal nanoribbon arrays. On the other hand, based on the commonly observed bundle-like nanoribbons at high-temperature deposition region, the well ordered nanoribbon arrays can be formed by a pushing transfer process. These results show the promising potential for the large-scale and high-efficiency fabrication of organic nanowire/nanoribbon transistors.

1.Introduction

The organic single crystal nanowire or nanoribbon transistors have attracted much attention because they are capable to combine the advantages of the single crystals and organic semiconductors, and overcome the difficulty of the growth of the large bulk crystal.[1-3] However, one challenging problem for organic single crystal nanowire/nanoribbon transistors is the nanoscaled device fabrication.[3] The small size of the nanowires/nanoribbons makes it difficult to handle the organic crystals, resulting in the low success ratio of the device fabrication and the time consumption. One solution to overcome such a challenge is to form the highly ordered and highly crystalline organic arrays on the substrate surface, which is desirable in organic electronics for the controlled, predictable assembly of devices and circuits.[4,5] It also shows a promising potential for high-efficiency and large-scale nanodevice fabrication.

Currently, most reports on the highly ordered organic nanowire/nanoribbon arrays focus on the solution method by the solvent evaporation, which is driven by a combination of dewetting, contact-line pinning, and self-assembly of the molecules.[6] The solution process requires organic semiconductors with good solubility in the solvents, which is not often the case and hence limits the application of the solution method for the growth of organic nanowire/nanoribbon crystals. In comparison, the vapor growth process is available for most organic materials, and it can produce higher-quality crystals and avoid the solvent pollution. Therefore, it is desirable to fabricate the organic nanowire/nanoribbon arrays based on the vapor process.

Metal phthalocyanines and phthalocyanine derivatives have been extensively studied for a variety of applications in organic electronics and optoelectronics. Among them, copper phthalocyanine (CuPc) and copper hexadecafluorophthalocyanine (F_{16}CuPc), which respectively behave as *p*- and *n*-type semiconductors, have attracted significant attention due to their high chemical stability and excellent electrical properties. The preparation of well-defined one dimensional (1D) nanostructures of CuPc and F_{16}CuPc is of considerable interest in the design of novel functional materials and nanoelectronic devices. Their single-crystalline nanoribbons have shown the high field-effect performance with the mobility of about 1 $cm^2V^{-1}S^{-1}$ for CuPc[7] and 0.35 $cm^2V^{-1}s^{-1}$ for F_{16}CuPc[8], respectively.

Here, we have studied in situ grown CuPc and F_{16}CuPc nanoribbon arrays via a vapor process and their formation mechanism, which possibly provides a feasible method to grow the arrays of other materials. On the other hand, the nanowire/nanoribbon bundle is a generally observed morphology for a variety of organic and inorganic nanowires.[9-18] Based on the nanowire/nanoribbon bundles, a pushing transfer method has been used to obtain the highly ordered nanoribbon arrays. Based on these nanoribbon arrays, one of the most difficult steps in the process of nanodevice fabrication, i.e., transferring the nanoribbon to the substrate, can be overcome, and the large-scale and high-efficiency fabrication of the nanoscaled organic field-effect transistors (OFETs) can be realized.

2. Experimental Section

The bundle-like nanoribbons and the in situ patterned nanoribbons of CuPc and F_{16}CuPc were grown with high reproducibility by a vapor-solid process. CuPc or F_{16}CuPc powder was put at the high-temperature zone of a horizontal tube furnace as the source material. The Si/SiO_2 substrate was used for the growth of in situ patterned nanoribbons, and the various substrates, such as glass, porous alumina, and Si/SiO_2 substrate, were used for the growth of bundle-like nanoribbons. The system was prepumped to ~15 Pa. Argon was introduced as a carrier gas

and was kept at a flow rate of 200 sccm. The control of the deposition region was a key factor for the formation of in situ grown nanoribbon and the bundle-like nanoribbons. The ultralong nanoribbons for two different morphologies can be obtained by further optimizing the growth time, deposition region, substrate material (porous Al_2O_3, Si, etc), and substrate treatment. The Si/SiO_2 was used as the transfer substrate for the formation of the array from the bundle-like nanoribbons. The transfer process was carried out by hand. CuPc and F_{16}CuPc nanoribbon OFETs were fabricated on Si/SiO_2 substrates. [19]

The morphology was characterized by scanning electron microscopy (SEM, Hitachi 4300) and transmission electron microscopy (TEM; JEOL 2010). The electrical measurements were carried out by a KEITHLEY 4200 system in a metallic shielded box at common temperature and pressure.

3. Results and discussion

3.1 Morphologies of in situ grown nanoribbon arrays and patterns

Figure 1 schematically shows the horizontal tube furnace for the vapor growth of CuPc and F_{16}CuPc, and the temperature distribution of the furnace for the growth of CuPc nanoribbons. When placing a substrate at the light blue region as shown in the temperature distribution image of Figure 1, the in situ grown CuPc nanoribbons on the surface of substrate can be formed. SEM images of Figure 2 clearly illustrate that an individual CuPc or F_{16}CuPc nanoribbon has a highly uniform width along its entire length with clean and smooth facets. The CuPc and F_{16}CuPc nanoribbons could be tightly adhered to the surface of the substrate during the growth for various architectures, as shown in Figure 2. The width of the in situ grown nanoribbon ranges from 40 to 150 nm and the length is from several to several tens of micrometers. Carefully observing the morphology of these nanoribbons, it is found that the in situ grown nanoribbons of CuPc and F_{16}CuPc mainly consist of two types of structures. The type I structure is presented in Figure 3a where the color of the nanoribbon is uniform and the whole nanoribbon tightly adheres to the surface of the substrate. The type II is presented in Figures 3b-e. The low- and high-magnification SEM images clearly show the bright and dark regions along the length of the nanoribbon. The contrast reveals the height fluctuation of the nanoribbon, which is caused by the change in the incident angle of the electron beam with respect to the nanoribbon surface.

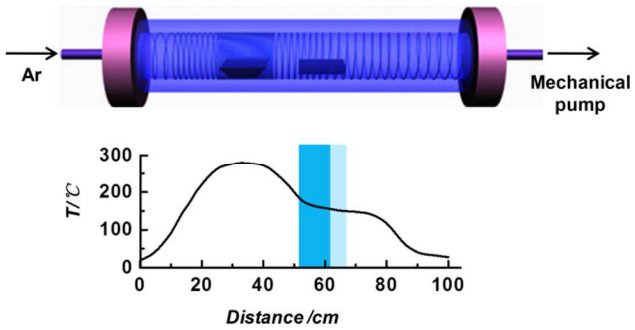

Figure 1. Schematic view of the horizontal tube furnace for the vapor growth of CuPc and F_{16}CuPc, and the temperature distribution of the tube furnace for the growth of CuPc nanoribbons. The bundle-like structures were fabricated in the sky blue region, and the in situ grown CuPc nanoribbons were obtained in the light blue region.

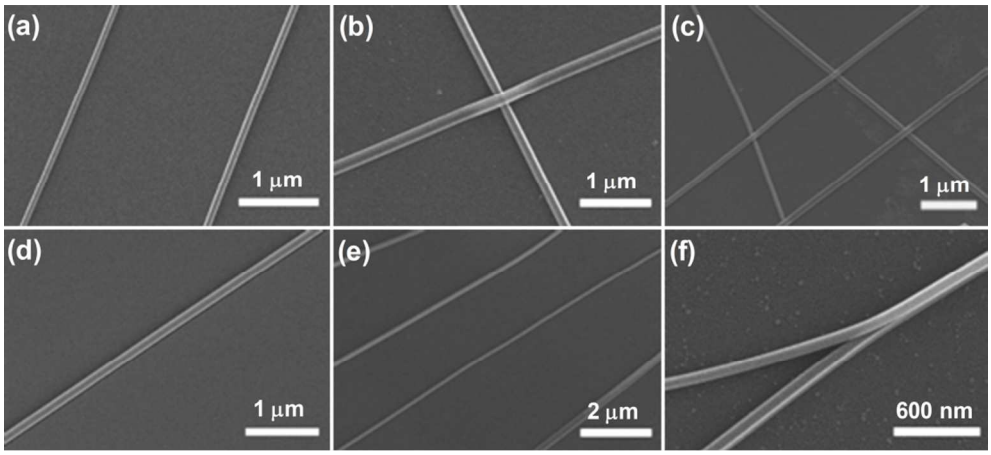

Figure 2. SEM images of in situ grown nanoribbons with different architectures: (a,b,c) CuPc, and (d,e,f) F_{16}CuPc.

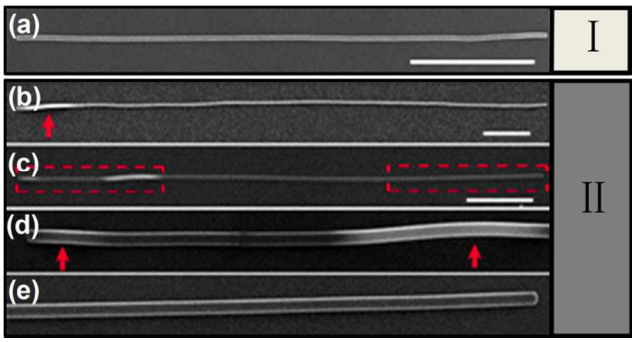

Figure 3. SEM images of in situ grown nanoribbons (a) structure of type I nanoribbon, and (b-e) structure of type II nanoribbon. Figures 3d and 3e are the enlargement of the boxed areas in Figure 3c. The arrowheads indicate the bright regions where the nanoribbons fail to adhere to the substrate. Scale bar: 2 μm.

3.2 Formation mechanism of the in situ grown nanoribbons

Based on the observed morphology, we take the CuPc as an example to analyze the growth process and mechanism in detail. Figure 4 schematically shows the formation of the in situ grown nanoribbon, and the corresponding SEM images. In the initial stage, the CuPc nanocrystals are formed on the substrate. Based on these nanocrystals as seeds, 1D CuPc nanoribbons are formed in the subsequent growth process. Because of the strong π-π interaction between CuPc moleculars along the [010] direction and the highest surface energy for (010) plane, the nanoribbons prefer to grow along the [010] direction.[20] The nanoribbons are likely to grow at a random angle with respect to the substrate. The preferred growth along the [010] direction makes the nanoribbon become longer and longer, and the aspect ratio increases. When the nanoribbon is short, the gravity of the CuPc nanoribbon and the van der Waals force between nanoribbon and substrate are weak. In this case, the nanoribbon remains straight, as shown in the schematic image of Figure 4a by the light purple ribbon. With the increasing reaction time, the length of the nanoribbon increases, and hence the gravity increases. The increased external moment caused by the gravity makes the bending occur, as shown in the schematic image of Figure 4a by the dark purple ribbon. When the nanoribbon is bent, due to the small thickness of the nanoribbon, the bending stresses distributed in the thickness direction are weak. Therefore, the nanoribbons possess high flexibility. As shown in Figures 4d-h, the nanoribbons can bend at 180° and even at 360° . Due to the excellent flexibility, the nanoribbons do not fracture but bend towards the substrate. The top or/and the middle sections of the nanoribbon preferentially contact with the surface of the substrate (Figures 4b_1 and 4b_2). The subsequent growth of the nanoribbon tightly adheres to the substrate and in situ grown nanoribbon (type II structure) can be obtained. Generally, the nanoribbon stands up on the substrate at a random angle in the initial growth stage. It is also possible that the initial angle is equal to zero, i.e., the nanoribbon is just parallel to the surface of the substrate. In this case, the whole nanoribbon remains tightly adhered to the surface of the substrate during the whole growth, forming type I structure. The amount of the type I structure should be much smaller than that of the type II structure since the angle is limited to zero for the type I structure. This is in good agreement with our observation in SEM measurements.

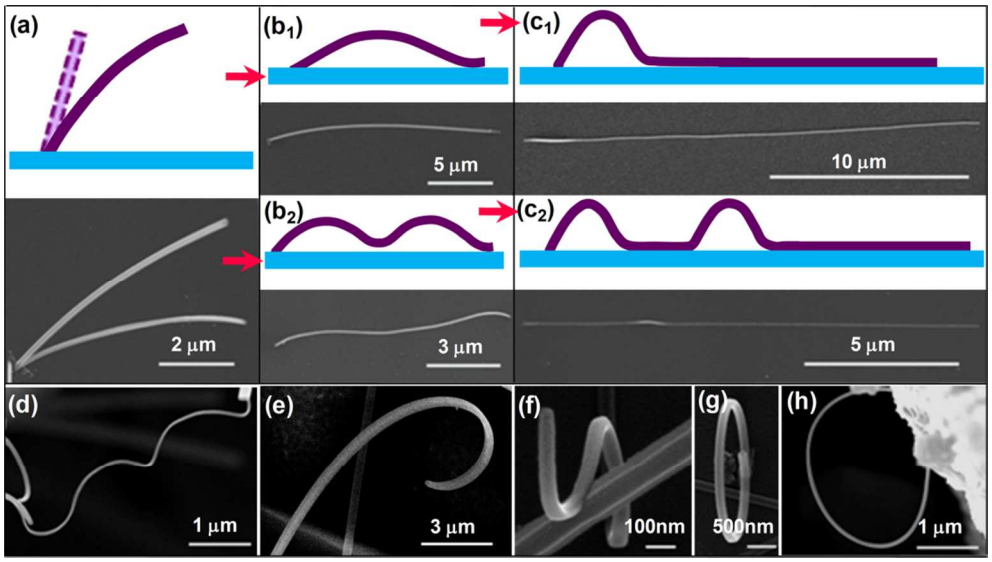

Figure 4. (a-c) Proposed growth process and corresponding experimental results showing the formation of in situ grown nanoribbons: (a) the tops of the nanoribbons are blurry due to their positions outside the depth of field, indicating that the nanoribbons are standing up on the substrate. (b_1) the top, and (b_2) the top and the middle sections of the nanoribbons adhere to the surface of the substrate driven by the gravity and the van der Waals force. (c_1,c_2) based on the top of the nanoribbons, they tightly adhere themselves to the substrate in the subsequent growth process. (d-h) SEM images of CuPc nanoribbons. The bending exhibits excellent flexibility of the nanoribbon.

The formation mechanism proposed here can also well explain the previous report that only the small-size nanoribbons can be in situ grown on the substrate.[21] With the increase in the thickness and the width of the nanoribbon, the limit bending moment increases.[22] They are not easily bent in the growth process by the gravity moment. Therefore, the in situ grown nanoribbon can not be formed based on large-size nanoribbon. The growth of small-size nanoribbons is a basic premise for the in-situ growth of the

ultralong nanoribbon. With the increasing thickness and the width of the nanoribbon, the internal moment increases.[22] In this case, the bent nanoribbon possibly recovers its original morphology once the external force is removed. This also explains why the larger-size nanoribbon shows the better elasticity as reported in the previous paper.[23]

The temperature distribution of the tube furnace for the growth of CuPc nanoribbon in Figure 1, shows that the bundle-like nanoribbons were formed in the high-temperature deposition region, and in situ grown nanoribbons were obtained in the lower-temperature region. In contrast, the productivity of in situ grown nanoribbons is far lower than that the bundle-like nanoribbons. Most of source material has been consumed because of the formation of a lot of bundle-like structures in the front end of the deposition region (sky blue region). The vapor concentration should be low at the low-temperature deposition region (light blue region). It facilitates the formation of the sparse small-size nucleation points, which combined with the low deposition temperature is favorable for the growth of the small-size nanoribbons, and the adherence of the nanoribbons onto the substrate surface in the subsequent growth process.

3.3. Morphology of bundle-like nanoribbons

At a high-temperature deposition region, the bundle-like structure nanoribbons with several tens of the individual nanoribbons jointed together at the bottom can be extensively observed. Typically, the bundle-like CuPc nanoribbons are formed in the sky blue region in the temperature distribution of Figure 1. Further, it is found that the bundle-like structure of the nanoribbons is easily formed in the experimental process. Figure 5 shows the SEM images of the CuPc and F_{16}CuPc bundles and their TEM images. The morphology characteristic implies that the nanocrystals have selectively aggregated onto the surface of the substrate at the initial stage and then the nanoribbon structures grow into bundles from the nucleation sites in various directions. The width of the bundle-like nanoribbon ranges from several tens of nanometers to several micrometers, and the length is from 20 to 100 micrometers. The selected area electron diffraction (SAED) patterns (insets of Figures 5c and 5e) reveal the good crystal quality of single crystal F_{16}CuPc and CuPc nanoribbons. The F_{16}CuPc ribbon grows along the [100] direction, and the CuPc ribbon grows along the [010] direction.[20,24] Generally, the formation of the bundle-like nanostructures originates from the kinetics dominant growth process. The nucleation and growth of the nanostructure is likely dominated to a larger extent by the kinetics process. The rapid growth velocity makes a large number of nanoribbons simultaneously grow based on one crystal nucleus, resulting in the formation of the bundle-like structure. It is found that a rougher substrate, for example, porous alumina or scratched silicon wafer, can improve the productivity of the bundle-like nanoribbons. The rough surface of the substrate provides the heterogeneous nucleation points which combines with the high deposition temperature resulting in the rapid growth rate in a un-equilibrium system[25].

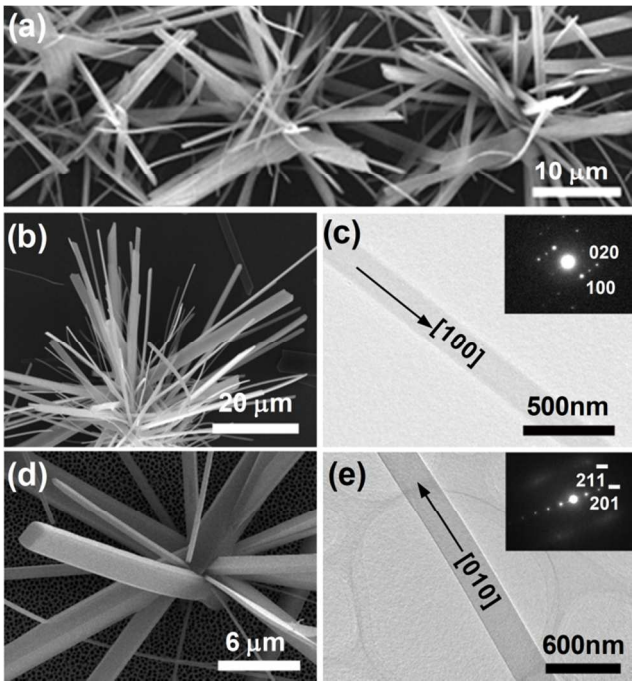

Figure 5. SEM and TEM images of the bundle-like nanoribbons: (a,b.c) F_{16}CuPc, and (d.e) CuPc. The insets are the corresponding SAED patterns.

3.4. Array formation from the bundle-like nanoribbons

From the view of devices, the in situ grown nanoribbons are preferred because it avoids the time-consuming transferring process of the nanoribbons and the interface pollution caused by the transferring process.[21] However, the productivity of the in situ grown nanoribbon is limited by the temperature fluctuation. Even a weak temperature fluctuation in the furnace possibly causes the failure of in situ growth of the nanoribbons. In comparison, the nanowire/nanoribbon bundle is a general observed morphology for a variety of organic and inorganic nanowires in both vapor and solution growth methods.[9-18] Obviously, the bundle-like nanoribbons are easily obtained with simpler growth condition control. If the nanoribbon arrays can be formed based on the bundle-like structure, the simple electrode fabrication process combined with the facile growth method makes the nanoscaled device fabrication dramatically accelerated. Here, a pushing transfer method is developed to realize the nanoribbon arrays according to the morphology characteristic of the bundle-like nanoribbons. As shown in Figure 6a, these nanoribbons stand on the substrate. A target substrate (Si/SiO_2) is placed over the standing nanoribbons and is gradually moved close to the nanoribbon bundles by hand. At the beginning, the top ends of some of nanoribbons contacts with the target substrate. When the target substrate moves downwards and forwards as shown in Figure 6b, these nanorbbons become bent first, and then the contact area between the individual nanoribbon and the target substrate is increased. This process makes more and more parts of an individual nanoribbon can be gradually flat adhered onto the target substrate. Finally, the forward movement also helps the bottom end of the nanoribbon to separate from the growth substrate, when the target substrate moves far away from the growth substrate (Figure 6c). Such a transfer process makes a few standing bundle-like nanoribbons adhered on the surface of the

target substrate in sparse distribution (Figures 6d-f). The transfer rate of the nanoribbons can be optimized by controlling the movement velocity of the target substrate, and the distance between the growth substrate and target substrate. This technique demonstrates the potential for large-scale fabrication of nanodevices, and is available for the other bundle-like organic and inorganic nanomaterials.

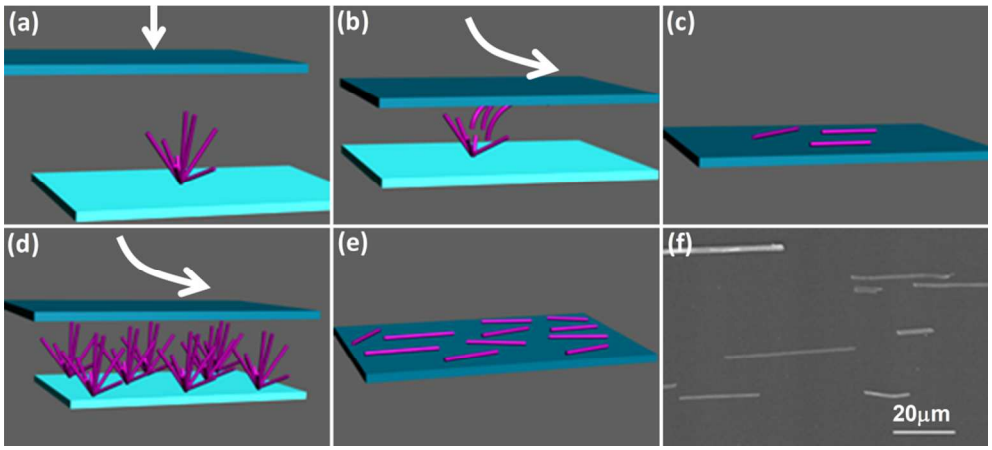

Figure 6. (a-c) Schematic images of pushing transfer method from a nanoribbon bundle. (d,e) Schematic images of nanoribon array formed from multiple nanoribbon bundles. (f) SEM image of a real nanoribbon array based on the nanoribbon bundles using the pushing transfer method.

3.5. Devices from the bundle-like nanoribbons

In order to show the promising potential of the nanoribbon array, we have fabricated the transistor devices based on the arrays formed from the bundle-like nanoribbons. By a gold-microwire electrode mask method, the nanoribbon devices can be fabricated.[20] The typical transfer characteristics of the CuPc and F_{16}CuPc transistors using the pushing transfer method are shown in Figures 7a and 7b. The devices are fabricated on the Si/SiO_2 substrate. The typical SEM images of the real devices are shown in the insets of Figure 7 (an optical microscopy image is shown in Supporting Information). The field-effect mobility (μ), on-off ratio, and threshold voltage are 0.01-0.5 $cm^2V^{-1}s^{-1}$, ~10^2-10^4 , -6--0.43 V for CuPc, and 0.0001-0.218 $cm^2V^{-1}s^{-1}$, ~10^2-10^4, -5.7-11 V for F_{16}CuPc, respectively. The histogram of Figure 7c shows the statistic results for the mobility of F_{16}CuPc by the pushing transfer method. The F_{16}CuPc exhibits the mobility inferior to CuPc, which mainly originates from the electron trapping at the semiconductor interface by hydroxyl groups in the case of commonly used SiO_2 dielectric.[26,27]

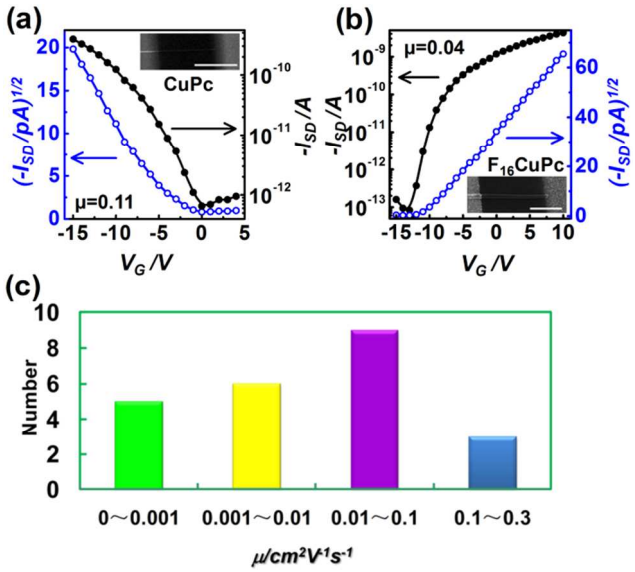

Figure 7. Electrical characteristics of the bundle-like nanoribbon transistors fabricated by the pushing transfer method: (a) Transfer curves of the CuPc nanoribbon transistor. (b) Transfer curves of the F_{16}CuPc nanoribbon transistor. (c) Mobility distribution of F_{16}CuPc nanoribbon transistors. Scale bar: 5 μm.

4. Conclusions

In situ patterned and bundle-like CuPc/F_{16}CuPc nanoribbons can be grown by the control of the deposition region and the deposition temperature. A low vapor concentration and a slow growth velocity facilitate the subsequent growth of nanoribbons following the previous length direction, resulting in the small-size long nanoribbons adhering onto the surface of the substrate. The fast growth velocity may cause a large number of nanoribbons to simultaneously grow on one crystal nucleus to form a bundle-like structure. The thickness and length of nanoribbons are also important for the growth of the in situ patterned nanoribbons. The thinner and longer nanoribbons tend to adhere to the surface of

the substrate due to the effect of gravity and their excellent flexibility. The thicker nanoribbons possess better elasticity. They are not easily bent, and hence can stand up on the substrate forming a bundle-like structure. Based on the bundle-like nanoribbons, the nanoribbon arrays can be formed by a pushing transfer method. The nanoribbon arrays show an outstanding advantage for high-efficiency and large-scale fabrication of nanodevices.

Acknowledgement

The authors acknowledge the financial support from NSFC (51103018, 51273036, 61376074, 51322305, 61261130092，51272238), Ministry of Science and Technology of China (2012CB933703), 111 Project (B13013), 2009 National Excellent Doctoral Dissertation Award from China (201024), the Program for New Century Excellent Talents of Ministry of Education (NCET-10-317), and Fundamental Research Funds for the Central Universities (11CXPY001, 12SSXM001).

Notes and references

[a] *Key Laboratory of UV Light Emitting Materials and Technology under Ministry of Education, Northeast Normal University, Changchun 130024, P. R. China*
E-mail: tangqx@nenu.edu.cn and tongyh@nenu.edu.cn
[b] *Beijing National Laboratory for Molecular Sciences Key Laboratory of Organic Solids, Institute of Chemistry Chinese Academy of Sciences, Beijing 100080, P. R. China*
E-mail: huwp@iccas.ac.cn

1 X. Fu, C. Wang, R. Li, H. Dong and W. Hu, *Sci China Chem,* 2010, **53**, 1225.
2 A. Briseno, S. Mannsfeld, S. Jenekhe, Z. Bao and Y. Xia, *Mater.Today*, 2008, **11**, 38.
3 Q. Tang, L. Jiang, Y. Tong, H. Li, Y. Liu, Z. Wang, W. Hu, Y. Liu and D. Zhu, *Adv. Mater.*, 2008, **20**, 2947.
4 W. Lu and C. M. Lieber, *Nat Mater.*, 2007, **6**, 841.
5 A. R. Tao, J. Huang and P. Yang, *Acc. Chem. Res.*, 2008, **41**, 1662.
6 Y. Tong, Q. Tang, H. T. Lemke, K. Moth-Poulsen, F. Westerlund, P.Hammershoj, K. Bechgaard, W. Hu and T. Bjornholm, *Langmuir*,2010, **26**, 1130.
7 R. Zeis, T. Siegrist and C. Kloc, *Appl. Phys. Lett.*, 2005, **86**, 022103.
8 Q. Tang, Y. Tong, H. Li and W. Hu, *Appl. Phys. Lett.*, 2008, **92**, 083309.
9 T. Lei and J. Pei, *J. Mater. Chem.*, 2012, **22**, 785.
10 J. H. Zhang, J. L. Wang, H. L. Wang, L. Jia, Z. K. Qu and Q. H. Kong, *Adv. Mater. Res.*, 2011, **284-286**, 2153.
11 J. Yin, J. Yan, M. He, Y. Song, X. Xu, K. Wu and J. Pei, *Chemistry*, 2010, **16**, 7309.
12 Lei Wang, Yan Zhou, Jing Yan, Jian Wang, J. Pei and Y. Cao, *Langmuir*, 2009, **25**, 1306.
13 T. Nakanishi, K. Ariga, T. Michinobu, K. Yoshida, H. Takahashi, T. Teranishi, H. Mohwald and G. D. Kurth, *Small*, 2007, **3**, 2019.
14 Fang Fang, Dongxu Zhao, Dezhen Shen, Jiying Zhang and B. Li, *Inorg. Chem.*, 2008 **47**, 398.
15 Z. Cheng, X. Chu, H. Zhong, Y. Kan, J. Yin and J. Xu, *Mater. Lett.*, 2013, **90**, 41.
16 Y. Han, X. Wu, Y. Ma, L. Gong, F. Qu and H. Fan, *CrystEngComm*, 2011, **13**, 3506.
17 V. R. Shinde, H. S. Shim, T. P. Gujar, H. J. Kim and W. B. Kim, *Adv. Mater.*, 2008, **20**, 1008.
18 R. H. Wang, C. M. Ruan, D. Kanayeva, K. Lassiter and Y. B. Li, *Nano Lett.*, 2008, **8**, 2625.
19 Q. Tang, H. Li, Y. Liu and W. Hu, *J. Am. Chem. Soc.*, 2006, **128**, 14634 .
20 Q. Tang, H. Li, M. He, W. Hu, C. Liu, K. Chen, C. Wang, Y. Liu and D. Zhu, *Adv. Mater.*, 2006, **18,** 65.
21 Q. Tang, H. Li, Y. Song, W. Xu, W. Hu, L. Jiang, Y. Liu, X. Wang and D. Zhu, *Adv. Mater.*, 2006, **18**, 3010.
22 K. H. Zhao and W. Y. Luo, *in Mechanics, Advanced Education Press: Beijing*, 1996, p220.
23 Q. Tang, Y. Tong, Y. Zheng, Y. He, Y. Zhang, H. Dong, W. Hu, T. Hassenkam and T. Bjornholm, *Small*, 2011, **7**, 189.
24 Y. Zhang, H. Dong, Q. Tang, S. Ferdous, F. Liu, S. C.B.Mannsfeld, W. Hu and A. L.Briseno, *J. Am. Chem. Soc.*, 2010, **132,** 11580
25 Y. H. Tong, Y. C. Liu, C. L. Shao and R. X. Mu, *Appl. Phys. Lett.*, 2006, **88**, 123111.
26 Y. Wen, Y. Liu, Y. Guo, G. Yu and W. Hu, *Chem. Rev.*, 2011, **111**, 3358.
27 R. P. Ortiz, A. Facchetti and T. J. Marks, *Chem. Rev.*, 2010, **110**, 205.

TOC

The highly ordered CuPc/F_{16}CuPc nanoribbon arrays have been formed via in situ vapor growth method and the pushing transfer method from the vapor-grown bundle-like nanoribbons.